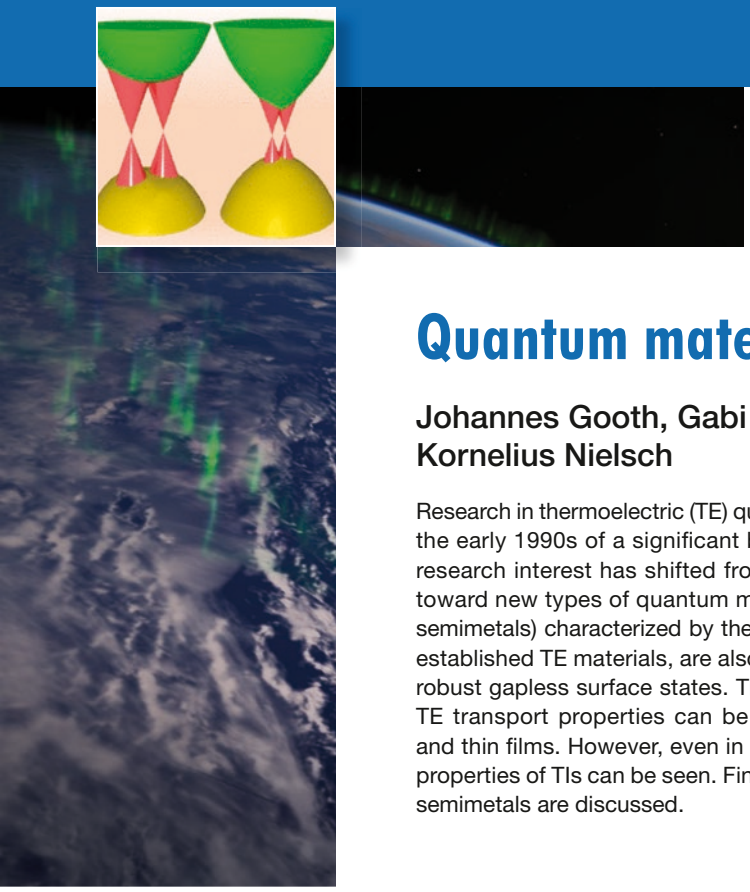


Quantum materials for thermoelectricity

Johannes Gooth, Gabi Schierning, Claudia Felser, and Kornelius Nielsch

Research in thermoelectric (TE) quantum structures was greatly propelled by the prediction in the early 1990s of a significant boost in TE efficiency by quantum size effects. Recently, research interest has shifted from quantum size effects in conventional semiconductors toward new types of quantum materials (e.g., topological insulators [TIs], Weyl and Dirac semimetals) characterized by their nontrivial electronic topology. Bi_2Te_3, Sb_2Te_3, and Bi_2Se_3, established TE materials, are also TIs exhibiting a bulk bandgap and highly conductive and robust gapless surface states. The signature of the nontrivial electronic band structure on TE transport properties can be best verified in transport experiments using nanowires and thin films. However, even in nanograined bulk, the typical peculiarities in the transport properties of TIs can be seen. Finally, the remarkable transport properties of Dirac and Weyl semimetals are discussed.

Introduction

The use of quantum size effects in semiconductor nanostructures strongly stimulated research on thermoelectricity over the past decade,[1–3] especially stimulated by the prediction of a significant boost in the thermoelectric (TE) figure of merit $ZT = (S^2 \sigma T)/(\kappa_{ph} + \kappa_{el})$ (S is the Seebeck coefficient, σ the electrical conductivity, κ the thermal conductivity with contributions from electrons and phonons, κ_{el} and κ_{ph}, and T absolute temperature) due to the transition from bulk to nanostructured materials by Hicks and Dresselhaus.[4,5] Quantum size effects lead to a modification of the energy levels of the charge carriers and enhance their kinetic energy. Additionally, classical size effects result in an enhanced surface scattering of electrons and phonons.

Topological insulators

Recently, research interest has shifted from quantum size effects in conventional/classical semiconductors to new types of quantum materials (e.g., topological insulators [TIs], Weyl and Dirac semimetals) characterized by their nontrivial electronic topological order. Topological order is a classification of matter by the internal structure of its quantum ground state. The class of TI materials hereby represents the most relevant quantum materials for thermoelectricity. Conventional semiconductors are characterized by a bulk band structure that is constituted by a valence band and a conduction band with parabolic bands and an energy bandgap $E_{gap} < 3$ eV. TE materials for near-room-temperature applications have this type of band structure, typically with E_{gap} around 0.1 eV to 0.25 eV for high performance in the low- to mid-temperature regime. TIs also exhibit this conventional bulk band structure of a semiconductor, but feature additional topological surface states with a linear dispersion relation. As in graphene, this results in relativistic carrier transport with extremely high carrier mobility, μ, and a small effective carrier mass, m_{eff}, which, in the ideal case, equals zero. Hence, in a primitive picture, TIs are characterized by graphene-like states on the surface of a conventional semiconductor. TIs therefore provide two different transport channels, one of graphene-like surfaces and the other of the (conventional) semiconducting bulk inner part.

Ordinary crystals are three-dimensional (3D) objects. If the crystal exhibits topological surface states completely surrounding the outer surface in all facet directions, this is called a 3D TI, also classified as a strong TI. If only certain or high-symmetry facets exhibit TI properties, the material is called a weak TI or topological crystalline insulator (TCI).

Topological surface states are protected from backscattering between equal and opposite momentum by time-reversal symmetry.[6] Therefore, the TI properties are robust, and they

Johannes Gooth, Max Planck Institute for Chemical Physics of Solids, Germany; Harvard University, USA; johannes.gooth@cpfs.mpg.de
Gabi Schierning, Leibniz Institute for Solid State and Materials Research Dresden (IFW Dresden), Germany; g.schierning@ifw-dresden.de
Claudia Felser, Max Planck Institute for Chemical Physics of Solids, Germany; claudia.felser@cpfs.mpg.de
Kornelius Nielsch, Leibniz Institute for Solid State and Materials Research Dresden (IFW Dresden), Germany; k.nielsch@ifw-dresden.de
doi:10.1557/mrs.2018.34

© 2018 Materials Research Society

https://doi.org/10.1557/mrs.2018.34 Published online by Cambridge University Press

not only are of theoretical interest, but also contribute to the materials' performance optimization. If, for instance, a surface of a 3D TI is oxidized, the TI states move deeper into the crystal, rather than being annihilated. Breaking of the TI state can be triggered by interaction with a magnetic dipole.[7] To probe for TI transport properties, experiments at high magnetic fields and low temperatures are performed to separate the contribution from the semiconducting bulk inner part of the material from the oscillatory behavior of the quantum transport caused by the mobile TI carriers of the surface states. By analyzing several quantum transport phenomena, such as weak antilocalization, the Aharonov–Bohm effect, Schubnikov–de Haas oscillations (SdH),[8] in addition to Fermi-level tuning, information about m_{eff} and μ can be obtained and the linear dispersion relation proven.

The link between TI and thermoelectricity is that good TE materials are usually narrow bandgap semiconductors (E_{gap} < 0.3 eV) and are constituted by heavy elements that suppress phonon propagation. The heavy elements also result in strong spin–orbit coupling. This is a prerequisite for the formation of topological surface states since it adds an amount of energy to the energy levels. If this amount is higher than the distance between the levels that define the bandgap, the band structure becomes inverted, and the topologically insulating state occurs.

Some of the best TE materials are also strong 3D TIs, for example, Bi_2Te_3, Bi_2Se_3, Sb_2Te_3,[9–11] and their solid solutions. Their macroscopic TE-transport properties exhibit signatures of the superposition of the surface and the bulk-transport channels. This is most clearly seen by studying transport properties in one-dimensional and two-dimensional model systems such as nanowires and thin films of Bi_2Te_3, Bi_2Se_3, and Sb_2Te_3.

In the last several years, substantial efforts have been invested in the development of TE Bi_2Te_3 nanowires and thin films to study the influence of a reduced dimension on the TE performance. The full *ZT* characterization of Bi_2Te_3 nanowires revealed values of *ZT* in the range of 0.02[12] up to 0.45,[13] considerably lower than the corresponding bulk *ZT* values (typically $ZT > 1$)[14] instead of higher as was predicted due to the beneficial effect of the reduced dimension.[5] This is not a general characteristic of nanowires. For instance, silicon nanowires exhibit *ZT* values between 0.6 and 1 at room temperature,[15,16] and perform therewith approximately one order of magnitude better than their bulk counterparts,[17,18] mostly due to increased scattering at the rough nanowire boundaries.[19] In InAs nanowires, a strong decrease in κ originates from increased phonon scattering at stacking faults between wurtzite and zincblende segments, accompanied by a reduction of σ attributed to a reduction of μ as a consequence of surface charges.[20,21]

In contrast, Bi_2Te_3, Bi_2Se_3, and Sb_2Te_3 exhibit a more metallic character with increasing surface-to-volume (*s*/*V*) ratio, as shown in **Figure 1**.[22–24] With higher *s*/*V*, a decrease in *S*, an increase in σ (not shown in Figure 1), and hence a decrease in *ZT* was evidenced. This can be interpreted to be a consequence of the surface states contributing charge carriers that exhibit superior μ carried under the regime of the linear dispersion relation. By analyzing Shubnikov-de Haas oscillations in Bi_2Te_3 nanowires,[23] it was found that the surface states have $m_c = 0.04\ m_0$ (the free electron mass), and $\mu = 21{,}000\ cm^2\ V^{-1}s^{-1}$. Shubnikov-de Haas oscillations are oscillations in the electrical resistivity of a material that occur at low temperatures in the presence of intense magnetic fields. The Shubnikov–de Haas effect is a macroscopic manifestation of the inherent quantum mechanical nature of matter. The transport properties can be described by a phenomenological

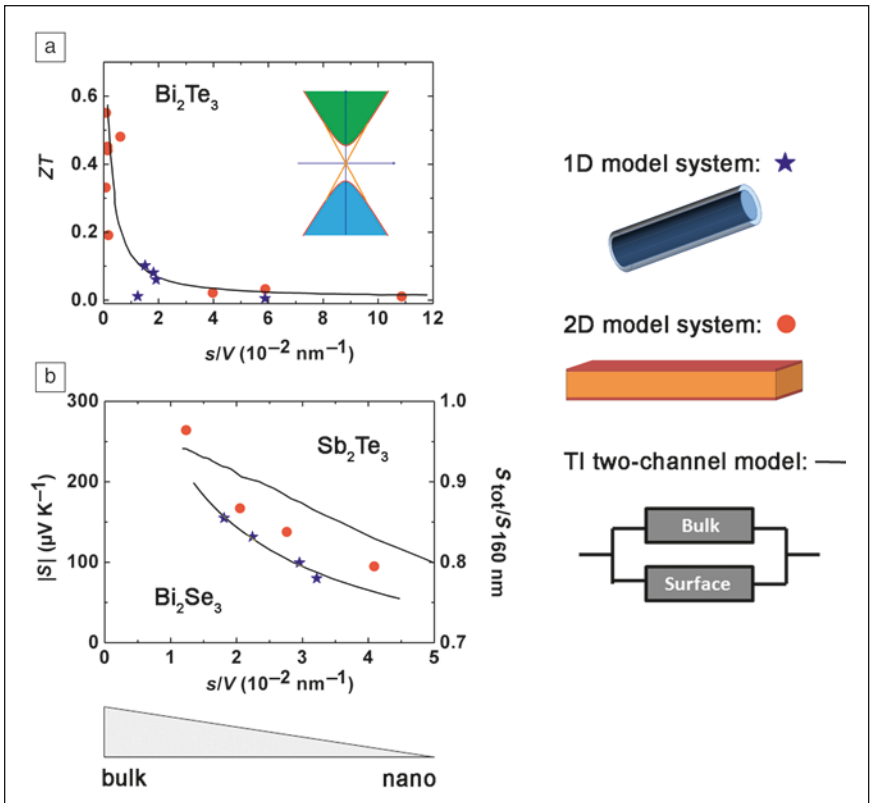


Figure 1. Compilation of thermoelectric (TE) transport data of the 3D topological insulator (TI) TE materials Bi_2Te_3, Sb_2Te_3, and Bi_2Se_3 obtained using 1D and 2D model systems (nanowires and thin films, respectively) with varying surface-to-volume (*s*/*V*) ratios. (a) *ZT* data of Bi_2Te_3 nanowires and thin films show a clear trend: The smaller *s*/*V*, the higher is *ZT*. Inset: Sketch of the band structure of a TI. It is constituted by a bulk valence (green) and conduction (blue) band that exhibits a parabolic dispersion, and features additional topological surface states that exhibit a linear dispersion. (b) Absolute Seebeck coefficients (*S*) of Bi_2Se_3 nanowires and normalized Seebeck coefficients of Sb_2Te_3 thin films show more metallic behavior with higher *s*/*V*.[22–24] Note: S_{tot}, measured total Seebeck coefficient with contributions from the bulk and the surface states; $S_{160\ nm}$, Seebeck coefficient measured using a thin film with 160-nm film thickness.

https://doi.org/10.1557/mrs.2018.34 Published online by Cambridge University Press

model that uses two in-parallel connected transport channels for surface and bulk and also by *ab initio* calculations.[24]

To date, the impact of topological surface states on nanograined bulk materials has not been fully understood. But some trends can be extracted. A breakthrough in TE materials development was the use of the ball-milling and hot-pressing method to achieve nanograined bulk with significantly improved *ZT*, compared to microstructured bulk, demonstrated for $Bi_{2-x}Sb_xTe_3$-alloys.[25] Today, this approach has been successfully applied to all known TE materials, systematically resulting in improved *ZT* values. It is remarkable that in $Bi_{2-x}Sb_xTe_3$ nanograined bulk, σ is higher than that for the microstructured bulk counterpart (see **Figure 2**a), although often only the lower κ is discussed.

Sun and coworkers[26] found an indication of the validity of interpreting this behavior as due to topological surface states. They analyzed the grain-size dependence of TE transport data in nanograined Bi_2Se_3. Due to its relatively high bandgap of 0.3 eV with an almost ideal linear electronic dispersion, called a Dirac cone, which results in exceptionally robust TI properties well above room temperature, Bi_2Se_3 is a perfect model TI.[9,27] As shown in Figure 2b, below an average grain size of 80 nm, *S* is lower and σ higher than in samples exhibiting an average grain size above this threshold. Most remarkable is the grain size-dependence of μ, with values of 400–600 $cm^2\ V^{-1}\ s^{-1}$ evidenced in nanograined Bi_2Se_3 for grain sizes below 80 nm, compared to around 12–15 $cm^2\ V^{-1}\ s^{-1}$ for samples with larger grain sizes. A higher σ of grain boundaries than that of the grain interiors is sometimes connected to a higher concentration of charge carriers. A higher μ of grain-boundary charge carriers is absolutely unique and can only be explained by the exceptional robustness of the surface states of strong 3D TIs that even survive the strongly distorted grain-boundary environment of a nanograined bulk.

TCIs are also found in the $Pb_{1-x}Sn_xTe$[28] (**Figure 3**) and $Pb_{1-x}Sn_xSe$[29] material families known for their massive Dirac states in three dimensions and exceptional TE properties[30,31] with record *ZT* values of 2.6, as in SnSe.[32] These materials can exhibit metallic surface states on high-symmetry crystal surfaces such as [111], [110], and [100] with an even number of Dirac cones.

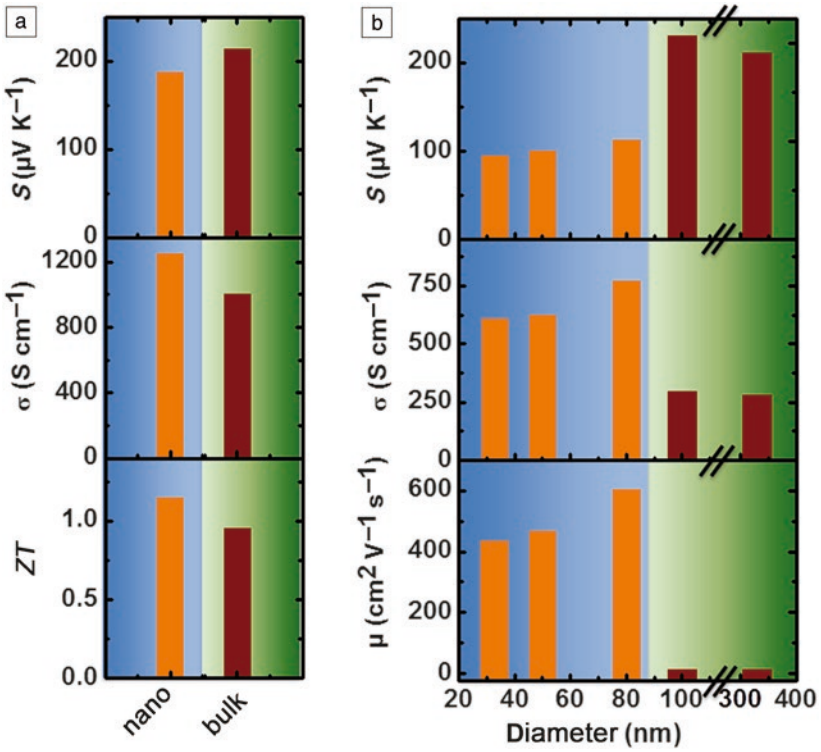


Figure 2. Signatures of topological insulator properties in nanograined bulk thermoelectric BiSbTe alloy and Bi_2Se_3. (a) Nanograined bulk of ball-milled and hot-pressed $Bi_{2-x}Sb_xTe_3$-alloy ingot resulted in an improved *ZT* value due to the often discussed reduction of the lattice thermal conductivity (not shown here), but also an enhancement in the electrical conductivity σ, accompanied by a reduction of the Seebeck coefficient *S*, despite the small grain sizes.[25] (b) Grain-size dependence of the electrical conductivity σ and the Seebeck coefficient *S* of Bi_2Se_3 nanograined bulk also demonstrates more metallic behavior with smaller grain sizes. The analysis reveals exceptionally high values of the charge-carrier mobility μ for average grain sizes below 80 nm.[26]

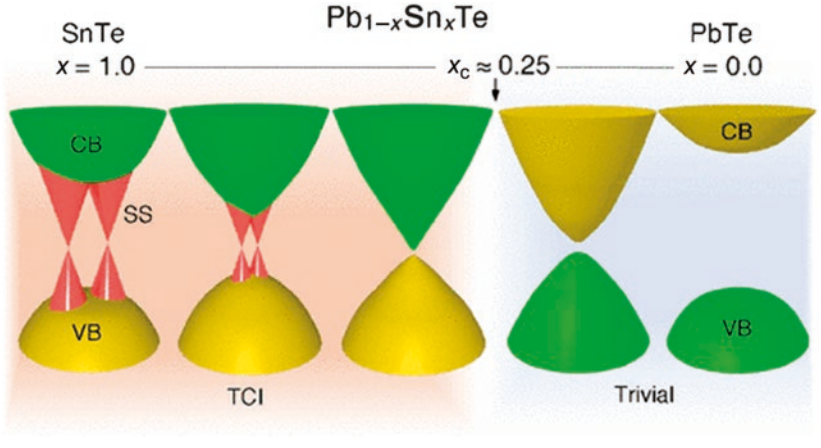


Figure 3. Nontrivial electronic topology in the $Pb_{1-x}Sn_xTe$ materials family. For $x = 0.4$, $Pb_{0.6}Sn_{0.4}Te$ is a Dirac semimetal. At the composition x_c, a trivial-to-nontrivial topological quantum phase transition between the topological crystalline insulator (TCI) phase and trivial phases occurs. This is also consistent with the band inversion taking place at x_c, visualized by the coloring of the valence band (VB, green in the trivial phases, yellow in the TCI phase) and conduction band (CB, yellow in the trivial phases, green in the TCI phase). Reprinted with permission from Reference 28. © 2013 Elsevier. Note: SS, surface state.

https://doi.org/10.1557/mrs.2018.34 Published online by Cambridge University Press

Dirac and Weyl semimetals

Dirac[33–35] and Weyl[36–39] semimetals, for instance, $Bi_{1-x}Sb_x$,[40,41] TaAs,[42] NbP,[43,44] or Cd_3As_2,[45–48] are two recently discovered classes of 3D topological materials in which conduction and valence bands touch linearly close to the Fermi energy. In Dirac semimetals, both time-reversal and inversion symmetries are preserved, and the Dirac cone is degenerated (**Figure 4**a). Weyl states emerge when one of these symmetries is broken. The discovery of Weyl semimetals has revitalized interest in Weyl fermions that were first discovered in high-energy physics experiments. The investigation of the TE transport properties of Weyl semimetals opens the door for an advanced understanding of these exotic states of matter[46] in which even Ohm's Law is fundamentally violated.[40]

As sketched in Figure 4b, the band touching point splits in momentum space into a pair of separated nodes (Weyl nodes) with opposite chirality, which refers to the handedness of the spin of electrons with respect to linear momentum. The conservation law of chirality dictates that the number of left-handed and right-handed electrons must always be symmetric, in other words, more electrons of one chirality than of the other cannot exist (Figure 4c). This symmetry has important consequences for the TE performance of Dirac and Weyl semimetals, because current flow is essentially the difference between the amount of left and right moving electrons of opposite chirality. Consequently, the net electrical current flow can be strongly suppressed due to the chiral conservation law. The thermopower, arising from the balance between the thermal diffusion current from hot to cold and its counter current from the accumulated charges at the cold side, is also strongly suppressed. Moreover, in both Dirac and Weyl semimetals, the energy spectrum is gapless, which results in ambipolar transport coefficients[49] such as a small S and enhanced κ_{el}. Therefore, Dirac and Weyl semimetals are naturally poor TE materials.

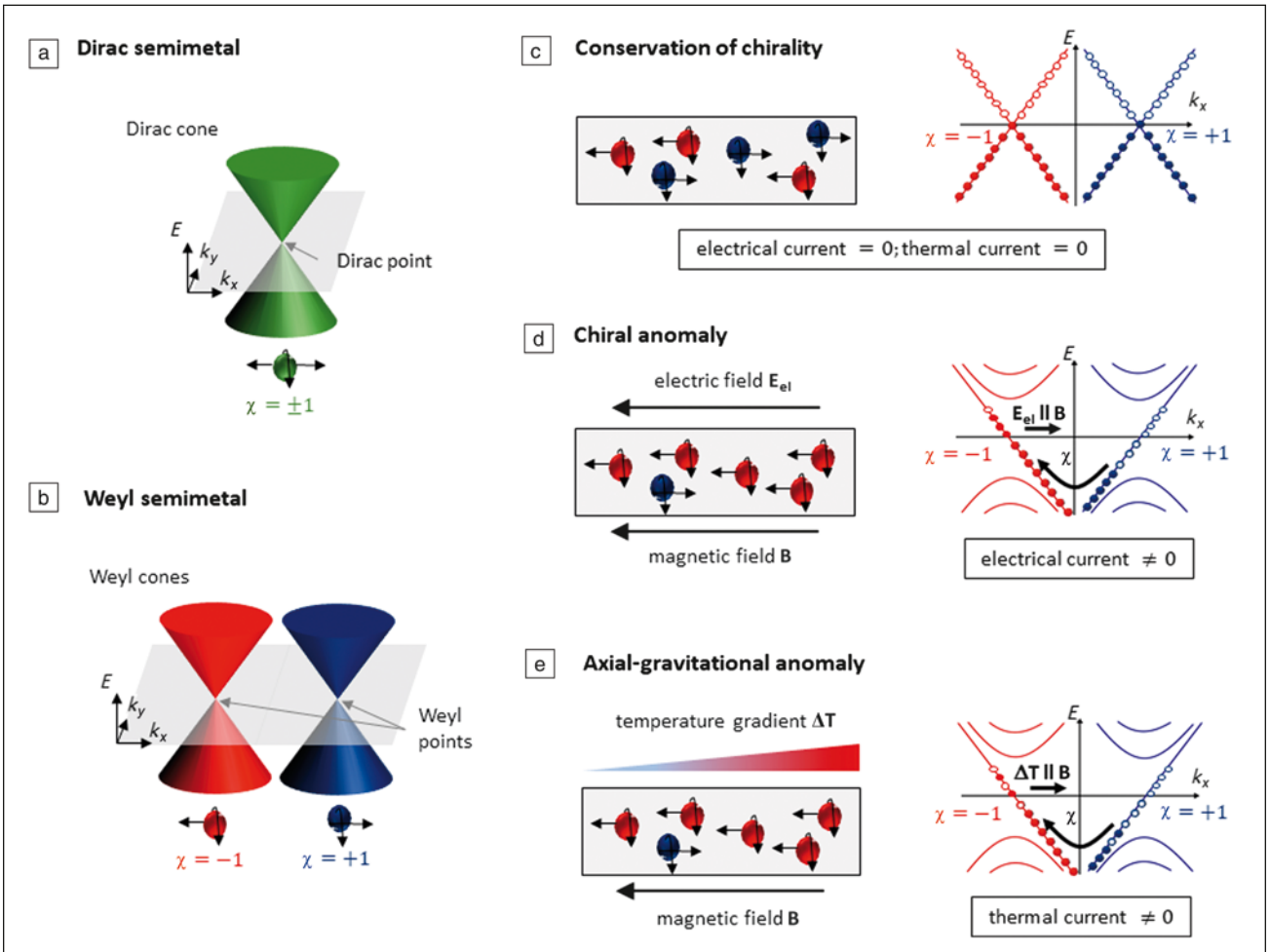


Figure 4. Dirac and Weyl semimetals. (a) Sketch of the band structure of a Dirac and (b) of a Weyl semimetal. The cones in a Dirac semimetal are degenerated in chirality χ (direction of the charge carrier's spin relative to its momentum). The Weyl semimetal hosts separated pairs of opposite chirality χ = −1 and χ = +1. E is the energy, and k_x, k_y are the momentum in the x and y directions, respectively. (c–e) show the real space scheme of the charge-carrier flow (left panels) and the associated band structure occupation (right panels). (c) Usually, the chirality is conserved. Consequently, net current flow is suppressed. However, quantum mechanical fluctuations can break the conservation law of chirality under (d) parallel magnetic **B** and electric fields $\mathbf{E}_{el}$ (chiral anomaly) and (e) parallel magnetic field **B** and temperature gradient $\Delta\mathbf{T}$ (axial-gravitational anomaly). Under these circumstances, electrical and thermal current flow is allowed and can be tuned by the applied magnetic field.

https://doi.org/10.1557/mrs.2018.34 Published online by Cambridge University Press

However, when a magnetic field is applied in parallel to an electric field, the chiral symmetry can be violated at the quantum level.[35,49–51] Applying electric and magnetic fields simultaneously to a Weyl semimetal leads to chiral charge pumping between the two branches of chiral energy levels (Landau levels), with a flow rate that is proportional to the product of the parallel magnetic and electric field components (Figure 4d). Likewise, a temperature gradient parallel to the magnetic field leads to an additional contribution that breaks the chiral symmetry (Figure 4e), originating from the so-called axial-gravitational anomaly.[43,52,53] The term "gravitational" refers to the fact that this quantum anomaly was originally thought to only occur in strong gravitational fields.[54] For all electronic TE transport coefficients, these quantum anomalies lead to an additional topological current in parallel to the bias aligned magnetic fields,[49,53] increasing S, σ, and κ_{el} of a Weyl semimetal with the square of the increasing magnetic field. Consequently, the TE performance of Dirac and Weyl semimetals may be strongly enhanced when magnetic fields are present. While the existence of the chiral[35,49–51] and the axial-gravitational anomaly[43] have recently been experimentally confirmed, a full ZT characterization of a Weyl semimetal in a magnetic field is still missing to date.

In addition to the anomalous longitudinal transport contributions, it has been found that the linear dispersion relations in Dirac and Weyl semimetals gives rise to a large perpendicular TE voltage, the Nernst signal,[29,55–57] which can exceed their thermopower by two orders of magnitude and is significantly larger than the thermopower of traditional TE materials. Such multiterminal TE devices are of special interest, because the heat reservoirs become spatially separated from the electrical circuitry, while at the same time performing at high efficiencies. In Weyl semimetals with tilted cones, so-called Weyl type II semimetals,[57] the Berry curvature, a local gauge field associated with the Berry phase of the topological band structure, is predicted to cause an anomalous Nernst effect even in the absence of a magnetic field, providing a platform for highly efficient TE energy converters. The Berry phase occurs in a quantum mechanical system during slow (adiabatic) traversing of a closed path in momentum space. The system does not return to its initial state, but its wave function acquires a phase factor, namely the Berry phase.

Conclusion

It seems no coincidence that many TE materials exhibit topological surface states or belong to other classes of materials with nontrivial electronic band structures. While the full spectrum of fascinating physical properties in these materials and their interplay with thermoelectricity are not yet fully understood, engineering the grain sizes and interfaces of these materials paves the path for advancing their TE performance.

Acknowledgments

This work was supported by Research Grant DFGRSF (NI616 22/1) "Contribution of topological states to the thermoelectric properties of Weyl semimetals."

References

1. M.S. Dresselhaus, G. Chen, M.Y. Tang, R.G. Yang, H. Lee, D.Z. Wang, Z.F. Ren, J.P. Fleurial, P. Gogna, *Adv. Mater.* **19** (8), 1043 (2007).
2. K. Nielsch, J. Bachmann, J. Kimling, H. Böttner, *Adv. Energy Mater.* **1** (5), 713 (2011).
3. C.J. Vineis, A. Shakouri, A. Majumdar, M.G. Kanatzidis, *Adv. Mater.* **22** (36), 3970 (2010).
4. L.D. Hicks, M.S. Dresselhaus, *Phys. Rev. B Condens. Matter* **47** (19), 12727 (1993).
5. L.D. Hicks, M.S. Dresselhaus, *Phys. Rev. B Condens. Matter* **47** (24), 16631 (1993).
6. J. Seo, P. Roushan, H. Beidenkopf, Y.S. Hor, R.J. Cava, A. Yazdani, *Nature* **466** (7304), 343 (2010).
7. S. Buchenau, P. Sergelius, C. Wiegand, S. Bäßler, R. Zierold, H.S. Shin, M. Rübhausen, J. Gooth, K. Nielsch, *2D Mater.* **4** (1), 015004 (2017).
8. J. Gooth, B. Hamdou, A. Dorn, R. Zierold, K. Nielsch, *Appl. Phys. Lett.* **104**, 243115 (2014), https://doi.org/10.1063/1.4883887.
9. H. Zhang, C.X. Liu, X.L. Qi, X. Dai, Z. Fang, S.C. Zhang, *Nat. Phys.* **5** (6), 438 (2009).
10. J.P. Heremans, R.J. Cava, N. Samarth, *Nat. Rev. Mater.* **2**, 17049 (2017).
11. N. Xu, Y. Xu, J. Zhu, *NPJ Quantum Mater.* **2** (1), 51 (2017).
12. J. Zhou, C. Jin, J.H. Seol, X. Li, L. Shi, *Appl. Phys. Lett.* **87** (13), 1 (2005).
13. C.L. Chen, Y.Y. Chen, S.J. Lin, J.C. Ho, P.C. Lee, C.D. Chen, S.R. Harutyunyan, *J. Phys. Chem. C* **114** (8), 3385 (2010).
14. G.J. Snyder, E.S. Toberer, *Nat. Mater.* **7** (2), 105 (2008).
15. A.I. Hochbaum, R. Chen, R.D. Delgado, W. Liang, E.C. Garnett, M. Najarian, A. Majumdar, P. Yang, *Nature* **451** (7175), 163 (2008).
16. A.I. Boukai, Y. Bunimovich, J. Tahir-Kheli, J.-K. Yu, W.A. Goddard III, J.R. Heath, *Nature* **451** (7175), 168 (2008).
17. S.K. Bux, R.G. Blair, P.K. Gogna, H. Lee, G. Chen, M.S. Dresselhaus, R.B. Kaner, J.-P. Fleurial, *Adv. Mater.* **19** (15), 2445 (2009).
18. G. Schierning, *Phys. Status Solidi A* **211** (6), 1235 (2014).
19. L. Liu, X. Chen, *J. Appl. Phys.* **107** (3), 033501 (2010).
20. S.F. Karg, V. Troncale, U. Drechsler, P. Mensch, P. Das Kanungo, H. Schmid, V. Schmidt, L. Gignac, H. Riel, B. Gotsmann, *Nanotechnology* **25** (30), 05702 (2014).
21. F. Zhou, A.L. Moore, J. Bolinsson, A. Persson, L. Fröberg, M.T. Pettes, H. Kong, L. Rabenberg, P. Caroff, D.A. Stewart, N. Mingo, K.A. Dick, L. Samuelson, H. Linke, L. Shi, *Phys. Rev. B Condens. Matter* **83** (20), 205416 (2011).
22. J. Gooth, J.G. Gluschke, R. Zierold, M. Leijnse, H. Linke, K. Nielsch, *Semicond. Sci. Technol.* **30** (1), 015015 (2015).
23. B. Hamdou, J. Gooth, A. Dorn, E. Pippel, K. Nielsch, *Appl. Phys. Lett.* **103** (19), 193107 (2013).
24. N.F. Hinsche, S. Zastrow, J. Gooth, L. Pudewill, R. Zierold, F. Rittweger, T. Rauch, J. Henk, K. Nielsch, I. Mertig, *ACS Nano* **9** (4), 4406 (2015).
25. B. Poudel, Q. Hao, Y. Ma, Y. Lan, A. Minnich, B. Yu, X. Yan, D. Wang, A. Muto, D. Vashaee, X. Chen, J. Liu, M.S. Dresselhaus, G. Chen, Z. Ren, *Science* **320** (5876), 634 (2008).
26. G.L. Sun, L.L. Li, X.Y. Qin, D. Li, T.H. Zou, H.X. Xin, B.J. Ren, J. Zhang, Y.Y. Li, X.J. Li, *Appl. Phys. Lett.* **106** (5), 053102 (2015).
27. Y. Xia, D. Qian, D. Hsieh, L. Wray, A. Pal, H. Lin, A. Bansil, D. Grauer, Y.S. Hor, R.J. Cava, M.Z. Hasan, *Nat. Phys.* **5** (6), 398 (2009).
28. Y. Tanaka, T. Sato, K. Nakayama, S. Souma, T. Takahashi, Z. Ren, M. Novak, K. Segawa, Y. Ando, *Phys. Rev. B Condens. Matter* **87** (15), 155105 (2013).
29. T. Liang, Q. Gibson, J. Xiong, M. Hirschberger, S.P. Koduvayur, R.J. Cava, N.P. Ong, *Nat. Commun.* **4**, 2696 (2013).
30. J.P. Heremans, V. Jovovic, E.S. Toberer, A. Saramat, K. Kurosaki, A. Charoenphakdee, S. Yamanaka, G.J. Snyder, *Science* **321**, 554 (2008).
31. Y. Pei, Z.M. Gibbs, A. Gloskovskii, B. Balke, W.G. Zeier, G.J. Snyder, *Adv. Energy Mater.* **4** (13), 1400486 (2014).
32. L.-D. Zhao, S.-H. Lo, Y. Zhang, H. Sun, G. Tan, C. Uher, C. Wolverton, V.P. Dravid, M.G. Kanatzidis, *Nature* **508** (7496), 373 (2014).
33. H. Li, H. He, H.Z. Lu, H. Zhang, H. Liu, R. Ma, Z. Fan, S.Q. Shen, J. Wang, *Nat. Commun.* **7**, 10735 (2016).
34. P.J.W. Moll, N.L. Nair, T. Helm, A.C. Potter, I. Kimchi, A. Vishwanath, J.G. Analytis, *Nature* **535** (7611), 266 (2016).
35. J. Xiong, S.K. Kushwaha, T. Liang, J.W. Krizan, M. Hirschberger, W. Wang, R.J. Cava, N.P. Ong, *Science* **350** (6259), 413 (2015).
36. C. Shekhar, A.K. Nayak, Y. Sun, M. Schmidt, M. Nicklas, I. Leermakers, U. Zeitler, Y. Skourski, J. Wosnitza, Z. Liu, Y. Chen, W. Schnelle, H. Borrmann, Y. Grin, C. Felser, B. Yan, *Nat. Phys.* **11** (8), 645 (2015).
37. P. Sergelius, J. Gooth, S. Bäßler, R. Zierold, C. Wiegand, A. Niemann, H. Reith, C. Shekhar, C. Felser, B. Yan, K. Nielsch, *Sci. Rep.* **6**, 33859 (2016).
38. S.Y. Xu, N. Alidoust, I. Belopolski, Z. Yuan, G. Bian, T.R. Chang, H. Zheng, V.N. Strocov, D.S. Sanchez, G. Chang, C. Zhang, D. Mou, Y. Wu, L. Huang, C.C. Lee, S.M. Huang, B. Wang, A. Bansil, H.T. Jeng, T. Neupert, A. Kaminski, H. Lin, S. Jia, M.Z. Hasan, *Nat. Phys.* **11** (9), 748 (2015).

https://doi.org/10.1557/mrs.2018.34 Published online by Cambridge University Press

39. A.C. Niemann, J. Gooth, S.C. Wu, S. Bäßler, P. Sergelius, R. Hühne, B. Rellinghaus, C. Shekhar, V. Süß, M. Schmidt, C. Felser, B. Yan, K. Nielsch, *Sci. Rep.* **7**, 43394 (2017).
40. D. Shin, Y. Lee, M. Sasaki, Y.H. Jeong, F. Weickert, J.B. Betts, H.-J. Kim, K.-S. Kim, J. Kim, *Nat. Mater.* **16** (11), 1096 (2017).
41. H.-J. Kim, K.-S. Kim, J.F. Wang, M. Sasaki, N. Satoh, A. Ohnishi, M. Kitaura, M. Yang, L. Li, *Phys. Rev. Lett.* **111** (24), 246603 (2013).
42. B. Peng, H. Zhang, H. Shao, H. Lu, D.W. Zhang, H. Zhu, *Nano Energy* **30**, 225 (2016).
43. J. Gooth, A.C. Niemann, T. Meng, A.G. Grushin, K. Landsteiner, B. Gotsmann, F. Menges, M. Schmidt, C. Shekhar, V. Süß, R. Hühne, B. Rellinghaus, C. Felser, B. Yan, K. Nielsch, *Nature* **547** (7663), 324 (2017).
44. U. Stockert, R.D. Dos Reis, M.O. Ajeesh, S.J. Watzman, M. Schmidt, C. Shekhar, J.P. Heremans, C. Felser, M. Baenitz, M. Nicklas, *J. Phys. Condens. Matter* **29**, (32), 325701 (2017).
45. T. Hosseini, N. Yavarishad, J. Alward, N. Kouklin, M. Gajdardziska-Josifovska, *Adv. Electron. Mater.* **2** (1), 1500319 (2016).
46. Z. Jia, C. Li, X. Li, J. Shi, Z. Liao, D. Yu, X. Wu, *Nat. Commun.* **7**, 13013 (2016).
47. C. Zhang, T. Zhou, S. Liang, J. Cao, X. Yuan, Y. Liu, Y. Shen, Q. Wang, J. Zhao, Z. Yang, F. Xiu, *Chin. Phys. B* **25** (1), 017202 (2015).
48. T. Zhou, C. Zhang, H. Zhang, F. Xiu, Z. Yang, *Inorg. Chem. Front.* **3** (12), 1637 (2016).
49. R. Lundgren, P. Laurell, G.A. Fiete, *Phys. Rev. B Condens. Matter* **90** (16), 165115 (2014).
50. X. Huang, L. Zhao, Y. Long, P. Wang, D. Chen, Z. Yang, H. Liang, M. Xue, H. Weng, Z. Fang, X. Dai, G. Chen, *Phys. Rev. X* **5** (3), 031023 (2015).
51. M. Hirschberger, S. Kushwaha, Z. Wang, Q. Gibson, S. Liang, C.A. Belvin, B.A. Bernevig, R.J. Cava, N.P. Ong, *Nat. Mater.* **15** (11), 1161 (2016).
52. K. Landsteiner, E. Megías, F. Pena-Benitez, *Phys. Rev. Lett.* **107** (2), 021601 (2011).
53. A. Lucas, R.A. Davison, S. Sachdev, *Proc. Natl. Acad. Sci. U.S.A.* **113** (34), 9463 (2016).
54. E. Witten, *Commun. Math. Phys.* **100** (2), 197 (1985).
55. G. Sharma, P. Goswami, S. Tewari, *Phys. Rev. B Condens. Matter* **93** (3), 035116 (2016).
56. T. Liang, J. Lin, Q. Gibson, T. Gao, M. Hirschberger, M. Liu, R.J. Cava, N.P. Ong, *Phys. Rev. Lett.* **118** (13), 136601 (2017).
57. Y. Ferreiros, A.A. Zyuzin, J.H. Bardarson, *Phys. Rev. B Condens. Matter* **96** (11), 115202 (2017). □



Johannes Gooth has been a joint postdoctoral fellow at the Max Planck Institute for Chemical Physics of Solids, Germany, and at Harvard University, since 2017. He studied physics at the University of Hamburg, Germany, and at Lund University, Sweden. After receiving his PhD degree from the University of Hamburg in 2014, he joined IBM Research–Zurich, Switzerland, as a postdoctoral researcher in 2015. He led the team that recently discovered the mixed axial-gravitational anomaly in Weyl semimetals. Gooth can be reached by email at johannes.gooth@cpfs.mpg.de.



Gabi Schierning joined the Leibniz Institute for Solid State and Materials Research Dresden (IFW Dresden), Germany, as head of the Department of Thermoelectric Materials in 2015. She received her PhD degree from University of Erlangen-Nuremberg, Germany, in 2005. After completing postdoctoral research, she led an independent research group at the University of Duisburg-Essen, Germany, from 2009 to 2015. She received the Award of Innovation of the State of North-Rhine Westphalia in the "young scientist" category in 2014. Schierning can be reached by email at g.schierning@ifw-dresden.de.



Claudia Felser has been director of the Max Planck Institute for Chemical Physics of Solids, Germany, since December 2011. She studied chemistry and physics at the University of Cologne, Germany, and received her PhD degree there in physical chemistry in 1994. After postdoctoral fellowships at the Max Planck Institute in Stuttgart and the CNRS in Nantes, France, she joined the University of Mainz, Germany, and became a full professor in 2003. She was a visiting scientist at Princeton University in 1999 and at Stanford University from 2009 to 2010, as well as a visiting professor at the University of Caen, France. Felser can be reached by phone at +49 351 4646-3000 or by email at claudia.felser@cpfs.mpg.de.



Kornelius Nielsch became director of the Leibniz Institute for Solid State and Materials Research Dresden (IFW Dresden), Germany, in 2015. He studied physics at the University of Duisburg, and completed his PhD degree at the Max-Planck-Institute Halle. In 2002, he was a postdoctoral associate at the Massachusetts Institute of Technology. Before he was appointed as professor for experimental physics by Hamburg University in 2006, he managed a research group in Halle. From 2009 to 2016, he coordinated the German Priority Program on Nanostructured Thermoelectrics. Nielsch can be reached by phone at +49 351 4659 102 or by email at k.nielsch@ifw-dresden.de.

JANIS

Cryogenic Wafer Probe Stations



- Applications include nano science, materials and spintronics
- 3.2 K - 675 K; high vacuum or UHV
- Up to 8 probes, DC to 67 GHz, plus fiber optics
- Zoom optics with camera and monitor
- Cooling options: liquid helium, liquid nitrogen or cryogen free
- Horizontal, vertical or vector magnetic field options are available

Contact us today:
sales@janis.com
www.janis.com/ProbeStations.aspx
www.facebook.com/JanisResearch

MRS Booth 306

https://doi.org/10.1557/mrs.2018.34 Published online by Cambridge University Press